

Peak shaving performance analysis of coal-fired units coupled with a molten salt-water heat storage system

Shenqiang Nie¹, Jianlong Ma^{1,2,3}*, Feng Wang¹, Xiaoming Dong¹, Qunhao Gu¹, Hongjie Su¹

¹ School of Energy and Power Engineering, Inner Mongolia University of Technology, Hohhot 010080, PR China

² Engineering Research Center of Renewable Energy at Universities of Inner Mongolia Autonomous Region, Hohhot 010080, PR China

³ Key Laboratory of Wind Energy and Solar Energy Technology, Ministry of Education, Hohhot 010080, PR China

* Corresponding author; E-mail: nishenqiang@163.com

With the rapid development of the renewable energy industry, thermal power units are increasingly required to provide peak shaving support within the power system. The integration of heat storage technology has emerged as a key strategy for enhancing the operational flexibility of coal-fired power units. However, existing solutions primarily rely on single-stage molten salt heat storage and release, which imposes limitations on overall heat storage capacity and efficiency. This study proposes a two-stage molten salt-water heat storage system and utilizes Epsilon simulation software to model a 660 MW coal-fired unit. Three different heat storage and release schemes for the coupled molten salt-water system are comparatively analyzed in terms of peak shaving performance and thermal efficiency. The results indicate that Scheme 1 (heat storage via main steam extraction) achieves the highest peak shaving performance. When the heat storage power is 120 MW, its peak shaving capacity reaches 60 MW. Scheme 3 (heat storage via intermediate-pressure cylinder exhaust extraction) exhibits the highest thermal efficiency, reaching 40.5% at a heat storage power of 40 MW, with the efficiency increasing as the storage capacity grows. When the heat release power is 50 MW, Scheme 1 demonstrates the highest thermoelectric conversion ratio (29.9%), while Scheme 3 records the lowest overall thermal efficiency (38.4%) and the highest coal consumption per unit of electricity generation (301.2 g/(kW·h)).

Key words: heat storage; peak shaving; coal-fired unit; thermal efficiency

Introduction

With the rapid advancement of the renewable energy sector, China's power system is transitioning toward a cleaner and low-carbon structure. However, the intermittency and unpredictability of renewable energy generation [1] present severe challenges to power supply stability. To facilitate the large-scale integration of renewable energy, coal-fired power plants have shifted from their traditional

role as the primary electricity provider to serving as critical supporting units for peak shaving [2]. Despite their pivotal role, conventional coal-fired units suffer from limited operational flexibility, sluggish load response, and constraints on peak shaving depth due to minimum boiler load requirements. These factors hinder their ability to meet the fast-response demands of modern power grids, highlighting the urgent need for flexible retrofitting solutions [3].

Existing strategies for improving the peak shaving capability of coal-fired power units primarily involve boiler and turbine modifications. On the boiler side, retrofitting measures include low-load burner optimization [4] and low-temperature flue gas heating [5], while turbine-side modifications include low-pressure (LP) cylinder zero output operation [6] and thermal storage via steam extraction. Among these methods, thermal storage technology has demonstrated several unique advantages, such as intertemporal energy utilization, long service life, and independence from geographical constraints [7]. As a result, it has become a mainstream solution for enhancing the operational flexibility of coal-fired units. In specific, molten salt and hot water heat storage [8] can be applied on a large scale to unit retrofitting to effectively improve peak shaving performance [9], offering broad application prospects. Thermal storage technology is typically incorporated into the thermal systems of coal-fired power plants, functioning as a 'linking hub'[10]. During periods of high renewable energy generation, surplus thermal energy from coal-fired units is stored to reduce electricity generation. Conversely, when renewable energy output decreases, the stored heat is released, reducing fossil fuel consumption and increasing power output [11].

In recent years, extensive research has been conducted on achieving flexible peak shaving in coal-fired power units through thermal storage technology. Liu *et al.* [12] investigated a 600 MW coal-fired unit and proposed eight molten salt heat storage schemes for peak shaving. Simulation results revealed that utilizing extracted exhaust of intermediate-pressure (IP) cylinder for molten salt heating, combined with a heat release strategy using molten salt to heat bypass feedwater, yielded the highest thermal efficiency and economic benefits. Jia *et al.* [13] employed Ebsilon software to analyze a 300 MW unit operating under industrial heat load conditions. By comparing three different thermal storage and release schemes, they observed that using main steam, reheat steam, and IP cylinder exhaust as heat storage sources enabled the greatest load variation. Moreover, when main steam and reheat steam served as heat storage sources, the system achieved the highest thermal storage efficiency. Felix Holy *et al.* [14] explored converting surplus electrical energy into high-exergy thermal energy for storage in high-temperature thermal storage devices. They further investigated the discharge process using a gas turbine within a Brayton cycle framework and conducted thermodynamic analyses on four different Brayton cycle configurations. Chen *et al.* [15] proposed a novel reheat steam extraction system that provides a viable approach for enhancing the operational flexibility of combined heat and power (CHP) plants and renewable energy systems. Wei *et al.* [16] examined the exergy efficiency of coal-fired units equipped with steam extraction-based molten salt thermal storage devices under 50% and 35% turbine heat acceptance (THA) conditions in the context of renewable energy integration. Wei *et al.* [17] studied an industrial extraction-condensing unit retrofitted with a steam bypass thermal storage system. By evaluating two heat release strategies, one for power generation and another for heating, they found that the combined peak shaving strategy involving bypass thermal storage achieved the largest peak shaving capacity. When the heating demand reached its maximum, the peak shaving capability of the modified system increased by 163.87 MW compared to the original unit. Abdur Rehman *et al.* [18] analyzed the integration of heat pumps and thermal energy storage in smart grids, district heating and cooling, and multi-energy carrier systems. The key technical characteristics and economic benefits of such

applications were analyzed in their study. Beiron *et al.* [19] developed a modeling framework that combines steady-state and dynamic process simulations with optimization models to assess the flexibility of CHP plants. By incorporating various electricity pricing scenarios, they evaluated the impact of thermal storage integration on power plant revenues. Meanwhile, Trojan *et al.* [20] designed a flexibility enhancement scheme for a 200 MW unit by installing a hot water storage tank. Their findings demonstrated that with a six-hour storage duration, the generator's power output could be reduced by 8.15% (15 MW).

The above studies have explored the feasibility of heat storage retrofitting for enhancing the flexibility of coal-fired power units. However, most research has focused on overall system design rather than separately analyzing heat storage and release schemes. In conventional designs, steam retains relatively high temperatures after being stored in molten salt, leading to incomplete utilization of its residual heat. In contrast, water, with its high specific heat capacity, good fluidity, and low corrosiveness, can effectively store the residual thermal energy from steam. Therefore, this study adopts a two-stage thermal storage and release strategy that integrates molten salt and water as heat storage media. Three heat storage schemes are proposed based on main steam extraction, reheat steam extraction, and IP cylinder exhaust extraction. Additionally, three heat release schemes are designed by matching molten salt heat release (hot section) with hot water heat release (cold section) at different heat release nodes. Using Ebsilon simulation software and a power plant model, this study compares the peak shaving capabilities of different heat storage and release schemes, providing a design framework for the flexible retrofitting of coal-fired power units.

Model building and validation

Coal-fired unit modelling

This study takes a 660 MW supercritical, single-reheat, single-shaft, three-cylinder, dual-exhaust, extraction-condensing unit as the research object. The unit is equipped with seven stages of extraction steam regenerative heating, comprising three LP heaters, one deaerator, and three high-pressure (HP) heaters. A thermodynamic model of the unit is developed using Ebsilon software, incorporating both design and off-design operating conditions. The fundamental system model is constructed, as shown in Fig. 1.

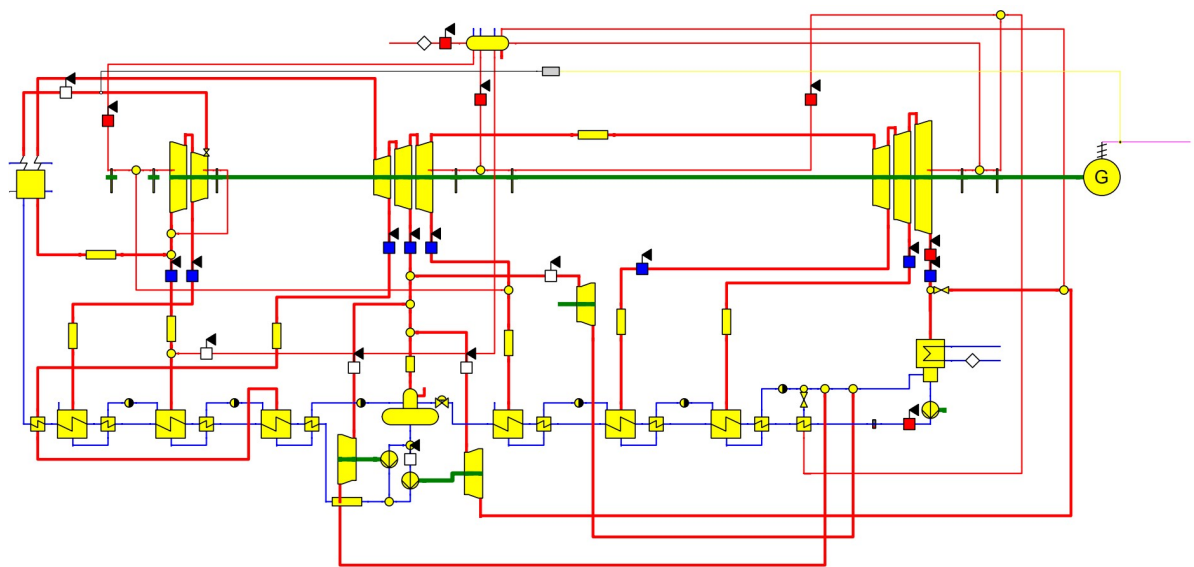


Fig.1 Schematic diagram of the unit model

To validate the model, thermal system off-design calculations are performed, followed by an error analysis for the 100% THA and 50% THA operating conditions. The comparison of simulated values and actual operational parameters is presented in Table 1. The maximum error observed is 2.2%, which falls within the acceptable range for engineering applications. These results confirm the model's suitability for off-design condition analyses.

Tab.1 Error analysis

parameters	Main Steam Flow Rate kg/s	Main Steam Enthalpy kJ/kg	Reheated Steam Flow Rate kg/s	Enthalpy of reheated steam kJ/kg	MP Exhaust Flow kg/s	MP Exhaust Enthalpy kJ/kg	unit output MW
100%THA simulation	558.5	3398.8	467.9	3589.6	347.2	3001.2	660
error	0	0.1%	0	0.1%	2.2%	0	0.1%
50%THA simulation	263.2	3524.2	231.4	3610.9	186.9	3034.8	330
error	0	0	1.2%	0	0.8%	0	0.2%

Heat storage-assisted peak shaving schemes

This study adopts the 50% THA operating condition as the baseline load. Different heat storage and release schemes are analyzed by aligning them with the original temperature and pressure conditions of the coal-fired unit. Three steam extraction-based heat storage schemes and three heat release schemes are designed for comparative analysis. For high-temperature heat storage (hot section), HITEC molten salt ($KNO_3+NaNO_2+NaNO_3$) is used, with an operating temperature range of 142–593°C. For low-temperature heat storage (cold section), hot water at 1 MPa gauge pressure is employed, with a corresponding saturation temperature of approximately 184°C. The specific heat storage and release schemes are outlined in Table 2.

The process flows of the heat storage and release schemes are illustrated in Figs. 2 and 3, respectively.

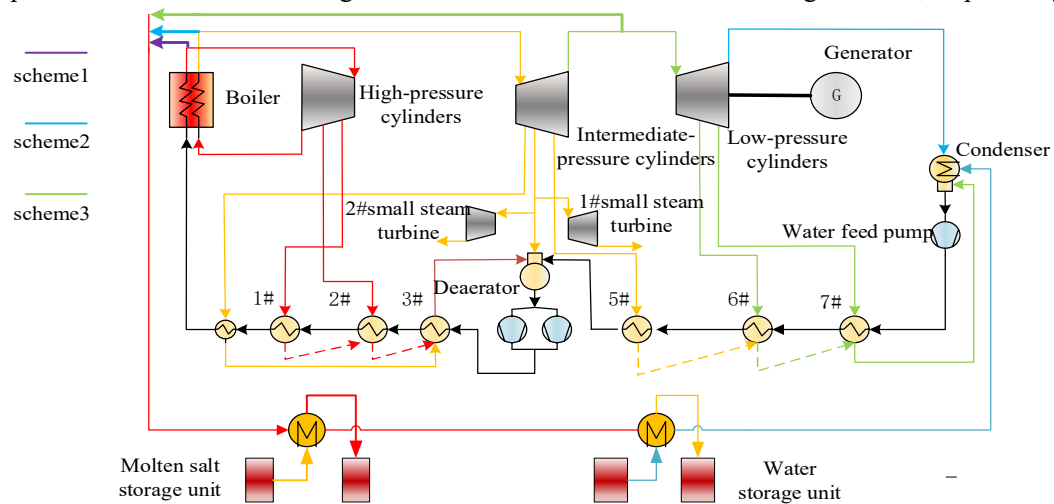


Fig.2 Heat storage schemes

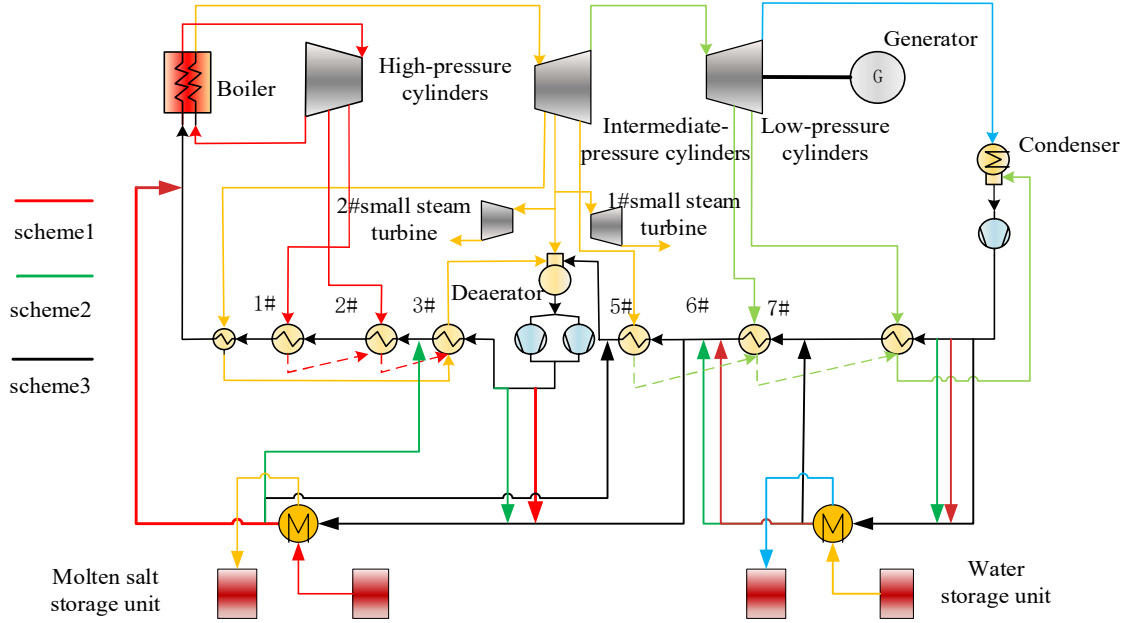


Fig.3 Heat release schemes

Tab.2 Heat storage and release scheme

Scheme	Heat storage scheme	Heat release scheme
1	Main steam extraction to condensate water	Hot section: deaerator outlet → boiler feedwater Cold section : feedwater pump outlet → 5# heater inlet
2	Reheat steam hot section pumping to condensate	Hot section: deaerator outlet → 2# heater inlet Cold section : feedwater pump outlet → 5# heater inlet
3	Medium Pressure Cylinder Outlet Pumping to Condensate	Hot section: 5# heater inlet → deaerator inlet Cold section : feedwater pump outlet → 6# heater inlet

Performance evaluation indicators

Thermal efficiency:

$$\begin{cases} \eta_c = \frac{P_c}{Q_{b1} - Q_c} \times 100\% (\text{heat storage phase}) \\ \eta_s = \frac{P_s}{Q_{b2} + Q_s} \times 100\% (\text{heat release phase}) \end{cases} \quad (1)$$

Where: η_c and η_s are the thermal efficiency during heat storage and heat release phases, %; P_c and P_s are the generated power during heat storage and heat release phases, kW; Q_{b1} and Q_{b2} are the boiler heat load during heat storage and heat release phases, kW; Q_c and Q_s are the heat storage capacity and heat release capacity of the thermal storage system, kW.

Coal consumption for power generation:

$$B = \frac{Q_b / \eta_b / q_{net}}{P} \times 3.6 \times 10^6 \quad (2)$$

Where: B is the coal consumption for power generation, g/(kW · h); η_b is the boiler combustion

efficiency, %; q_{net} is the net calorific value of the fuel, kJ/kg; P is the generation power, kW.

Peak shaving capacity and depth:

Peaking capacity and depth during heat storage :

$$\Delta P_c = P_0 - P_e, \varepsilon_c = \frac{\Delta P_c}{P_e} \times 100\% \quad (3)$$

Peaking capacity and depth during heat release :

$$\Delta P_s = P_s - P_0, \varepsilon_s = \frac{\Delta P_s}{P_e} \times 100\% \quad (4)$$

Where: ΔP_s and ΔP_c are the peaking capacity during heat storage and heat release phases, MW; P_0 and P_e are the rated power output of the unit at 50% THA and 100% THA, MW; ε_c and ε_s are the peak shaving depth during heat storage and heat release phases, %.

Thermoelectric conversion ratio:

$$\partial = \frac{P_c - P_0}{Q_s} \times 100\% \quad (5)$$

Where: ∂ is the ratio of increased power output to heat released by the storage system, %.

Results and analysis

Heat storage process analysis

The heat storage power is set to 40 MW, 80 MW, and 120 MW, respectively, and the corresponding heat storage capacities are shown in Fig. 4. A comparison of the peak shaving capacity and peak shaving depth achieved under different heat storage power levels for the three heat storage schemes is presented in Figs. 5 and 6, respectively. Additionally, Table 3 provides the key steam extraction node parameters for each scheme during the heat storage phase.

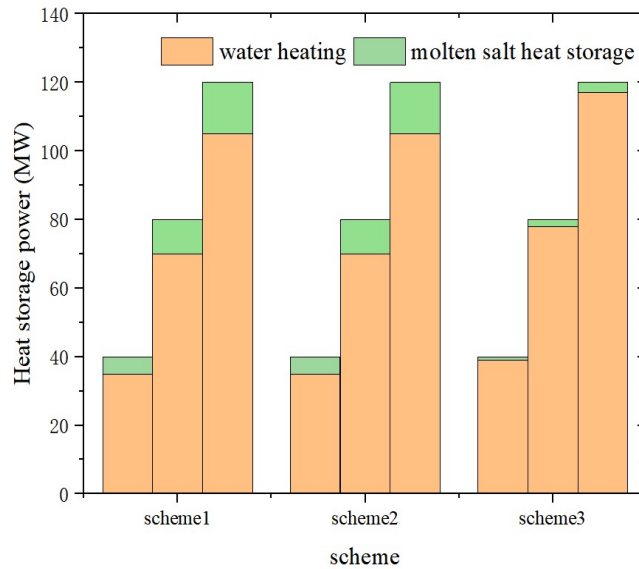


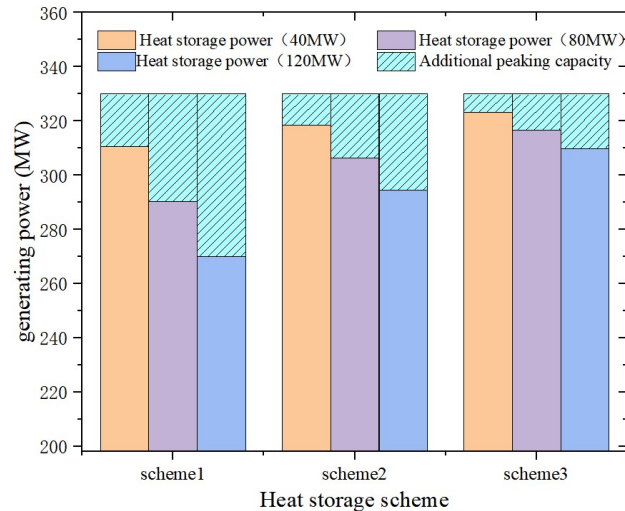
Fig.4 Heat storage variation under different heat storage schemes

Tab.3 Steam extraction node parameters

Scheme	Extraction node	Temp /°C	Pressure /bar
1	Mains steam	566	118.5
2	Reheat steam (hot section)	566	24.2
3	IP cylinder exhaust	283.3	3.3

Peak shaving capacity and depth

As the heat storage power increases from 40 MW to 120 MW, the unit's power generation gradually decreases across the three schemes. This occurs because a greater heat storage capacity reduces the thermal energy available for turbine operation, thereby effectively lowering the unit's power output and enhancing its peak shaving capability. Among the three schemes, Scheme 1 achieves the highest peak shaving capacity and depth, reaching 60 MW when the heat storage power is 120 MW. A comparative analysis reveals that the incremental peak shaving capacity remains nearly unchanged across the three schemes, but the overall peak shaving performance follows the order of Scheme 1 > Scheme 2 > Scheme 3. This trend is primarily attributed to the common extraction steam-based heat storage strategy employed in all three schemes, where the extracted steam is condensed in the condenser after heat storage. For example, at a heat storage power of 40 MW, the peak shaving capacities of the three schemes are 19 MW, 11 MW, and 6.7 MW, with peak shaving depths of 3%, 1.7%, and 1%, respectively. The superior performance of Scheme 1 (heat storage via main steam extraction) can be attributed to the higher energy quality of the extracted steam, its stronger ability to perform work inside the turbine, and a longer expansion process. In contrast, the extraction of reheat steam and IP cylinder exhaust prevents the steam from performing work in the IP and LP cylinders or only in the LP cylinder. Although Scheme 1 extracts a relatively lower amount of steam at the same heat storage power, it still reduces the turbine's work output more effectively, resulting in the greatest load reduction and highest peak shaving depth.

**Fig.5 Peaking shaving capacity under different heat storage schemes**

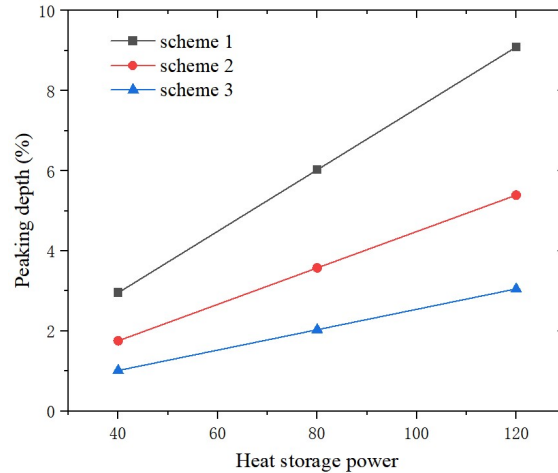


Fig.6 Peaking shaving depth under different heat storage schemes

Thermal efficiency and coal consumption for power generation

Figs. 7 and 8 illustrate the comparison of the thermal efficiency and coal consumption rate under different heat storage schemes. The figures indicate that at 50% THA, the original thermal efficiency of the coal-fired unit is 39.5%. All three heat storage schemes achieve higher thermal efficiency than the original unit. Furthermore, within the same heat storage scheme, thermal efficiency increases as the heat storage capacity rises. Taking Scheme 1 as an example, extracting part of the steam effectively reduces condensation losses in LP cylinder exhaust. The greater the heat storage capacity, the more the exhaust losses decrease, thereby improving the overall efficiency. A comparison of the three schemes uncovers that under the same heat storage power, the unit's thermal efficiency ranks from high to low as Scheme 3 > Scheme 2 > Scheme 1. This is because the work efficiency of steam within the turbine is generally above 90%. Scheme 3 requires extracting more steam under the same heat storage power, which not only reduces LP cylinder exhaust losses but also allows the steam to perform work in the HP and IP cylinders, resulting in relatively higher unit efficiency. At 50% THA, the original unit's coal consumption for power generation is approximately 310.3 g/(kW·h). However, the coal consumption per unit of electricity generation increases in all three heat storage schemes. Taking Scheme 1 as an example, under heat storage loads of 40 MW, 80 MW, and 120 MW, the coal consumption per unit of electricity generation is 330, 352.7, and 378.1 g/(kW·h), respectively. Under the same heat storage power, the coal consumption per unit of electricity generation follows the order of Scheme 1 > Scheme 2 > Scheme 3. This is because the extracted steam in Scheme 1 has a higher energy quality compared to Scheme 2 and Scheme 3. Since this steam is directly extracted without performing work for power generation, the energy loss per unit of electricity generation increases, leading to a rise in corresponding coal consumption. For the same scheme, the coal consumption per unit of electricity generation increases proportionally with heat storage capacity. This is because the thermal efficiency of the steam turbine remains around 90%, meaning the energy loss per unit of electricity generation follows a nearly fixed proportion, increasing with the rise in heat storage capacity.

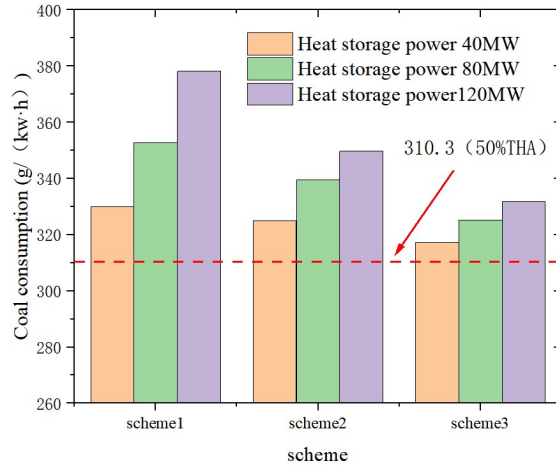


Fig.7 Coal consumption per unit of electricity generation under different heat storage schemes

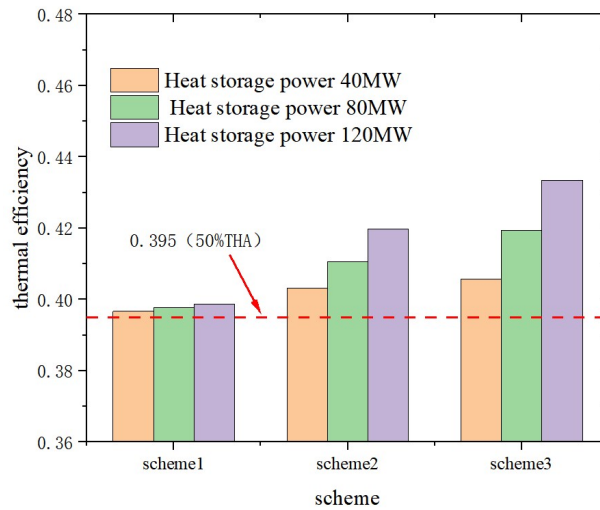


Fig.8 Thermal efficiency under different heat storage schemes

Heat release process analysis

The heat release schemes adopt a method in which high-temperature molten salt and low-temperature water tanks release heat separately. The heat release power is set at 10, 20, 30, 40, and 50 MW, with the corresponding composition of heat release power shown in Fig. 9. A comparison of the peak shaving capacity and the thermoelectric conversion ratio for the three heat release schemes at different heat storage power levels is presented in Figs. 10 and 11. The key heat release node parameters are summarized in Table 4.

Tab.4 Heat release node parameters

Scheme	Molten salt (high temperature)				Water (low temperature)			
	Cold water pressure /bar	Cold water temp /°C	Hot water pressure /bar	Hot water temp /°C	Cold water pressure /bar	Cold water temp /°C	Hot water pressure /bar	Hot water temp /°C
1	118.9	153	118.5	244	31	46	30.9	95
2	118.9	153	118.7	185	31	46	30.9	95
3	30.8	98	30.7	133	31	46	30.9	57

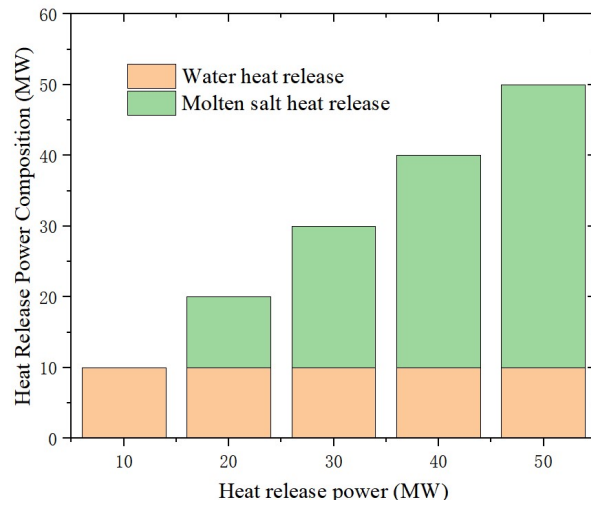


Fig.9 Composition of heat release power

Peak shaving capacity and thermoelectric conversion ratio

When the heat release power is 10 MW, only the low-temperature water tank participates in heat release. The power generation of the unit increases in all three heat release schemes, but the up-peaking capacity of Scheme 1 and Scheme 2 is 1.3 MW, with a thermoelectric conversion ratio of 13%, both of which are higher than those of Scheme 3. This is because all three heat release schemes use the thermal storage device to heat the feedwater, thereby reducing turbine extraction steam volume, increasing the unit's work output, and improving power generation. At the same heat release power, Scheme 1 and Scheme 2 bypass both the 6# and 7# regenerative heaters, thus reducing extraction steam from two turbine stages, whereas Scheme 3 only bypasses the 7# regenerative heater. Compared to Scheme 3, the heat release process in Scheme 1 and Scheme 2 eliminates 6# extraction steam, which has a higher energy quality and stronger work potential in the turbine. As a result, these schemes exhibit better up-peaking capability and higher thermoelectric conversion ratios at the same heat release power.

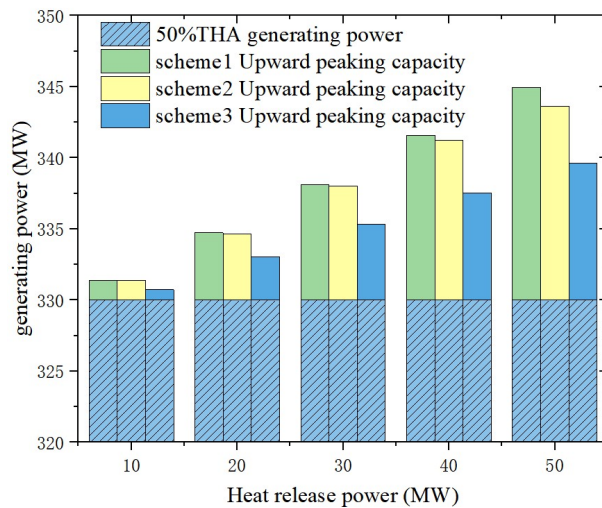


Fig.10 Up-peaking capacity under different heat release schemes

As the heat release power increases, the unit's up-peaking capacity also rises, following the order of Scheme 1 > Scheme 2 > Scheme 3. Additionally, the performance gap between the three schemes widens with increasing heat release power. When the heat release power reaches 50 MW, the peak shaving capacities of the three schemes are 15 MW, 13.6 MW, and 9 MW, respectively.

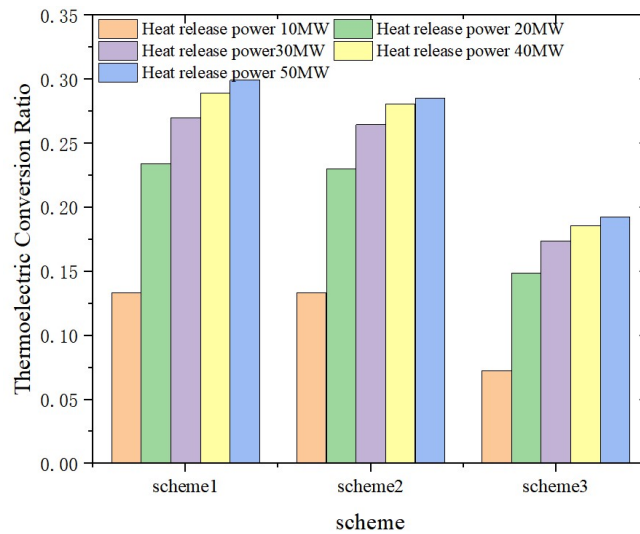


Fig.11 Thermoelectric conversion ratio under different heat release schemes

When the heat release power reaches 50 MW, the thermoelectric conversion ratios for the three schemes are 30%, 27%, and 19%, respectively. This difference stems from the varying high-temperature heat release nodes among the schemes. Scheme 1 reduces HP cylinder steam extraction while increasing the reheat steam volume, allowing more high-quality energy to perform work. Scheme 2 only reduces the extraction steam volume of the 3# regenerative heater, whereas Scheme 3 only reduces that of the 5# regenerative heater. Since the energy quality of the extracted steam decreases in this order, Scheme 1 achieves the highest thermoelectric conversion ratio and the greatest up-peaking capacity. Considering both high-temperature and low-temperature heat release, the closer the cold water extraction node is to the feedwater system and the closer the hot water input node is to the boiler (signifying more extraction steam regenerative heating stages are bypassed), the higher the thermoelectric conversion ratio and peak shaving capacity, leading to better peak shaving performance.

Thermal efficiency and coal consumption for power generation

Figs. 12 and 13 compare the unit's thermal efficiency and coal consumption rate under the three different heat release schemes. The figures indicate that thermal efficiency decreases in all cases when heat is released, and the higher the heat release power, the lower the thermal efficiency. This is mainly due to the increased condensation heat loss in the LP cylinder exhaust as the thermal storage system releases heat.

At a heat release power of 10 MW, the thermal efficiency of Scheme 1 and Scheme 2 is equal at 39.3%, while Scheme 3 has the lowest efficiency at 39.2%. This is because, despite the increased exhaust condensation loss, Scheme 1 and Scheme 2 allow more high-quality energy to perform work, thus generating more electricity than Scheme 3. Consequently, the coal consumption per unit of electricity generation for Scheme 1 and Scheme 2 is lower than that for Scheme 3.

As the heat release power rises, the differences in thermal efficiency and coal consumption rate among the three schemes become more pronounced. This is because, with increasing high-temperature heat release, Scheme 1 gradually replaces more high-quality turbine extraction steam. Given that the power generation potential of the extracted steam in Scheme 1 exceeds that of Scheme 2 and Scheme 3, this advantage becomes even more evident at higher heat release power levels. At a heat release power of 50 MW, the thermal efficiencies of the three schemes are 38.9%, 38.7%, and 38.4%, respectively. However, these efficiency gains are still insufficient to offset the heat loss caused by increased exhaust condensation losses. As external heat release replaces turbine extraction steam for regenerative heating, more steam remains available for work. Consequently, although the thermal efficiency gradually declines with increasing heat release power, the coal consumption rate decreases. For instance, in Scheme 1, the coal consumption per unit of electricity generation decreases from 308.8 g/(kW·h) to 297 g/(kW·h) as the heat release power increases. At a heat release power of 50 MW, the coal consumption per unit of electricity generation for the three schemes is 297, 299.5, and 301.2 g/(kW·h), respectively. This trend occurs because the higher the energy quality of the heat from the thermal storage system that replaces turbine extraction, the greater the steam's work potential and the higher the power generation, ultimately resulting in the lower coal consumption rate in Scheme 1.

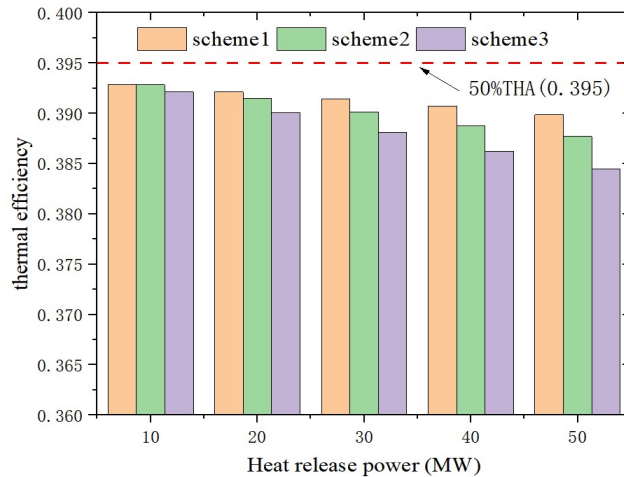


Fig.12 Thermal efficiency under different heat release schemes

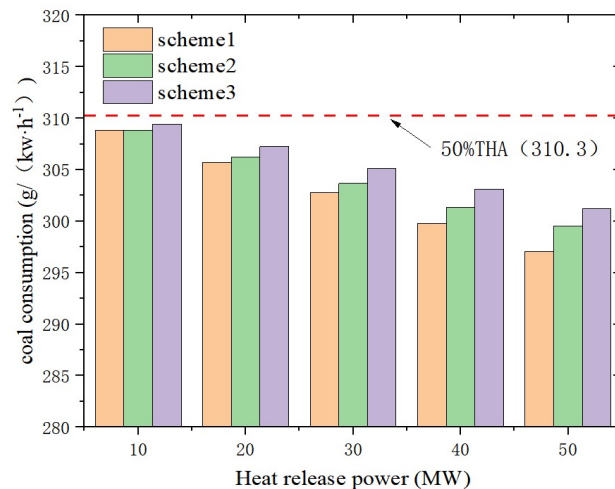


Fig.13 Coal consumption per unit of electricity generation under different heat release schemes

Conclusion

Enhancing the peak shaving flexibility of coal-fired power units is currently a research hotspot. This study focused on a 660 MW coal-fired power unit and employed Ebsilon software to simulate peak shaving retrofitting schemes for thermal power units under 50% THA operating conditions. Without modifying the original unit's node parameters, a comparative analysis was conducted on the thermodynamic performance and peak shaving performance of three heat storage schemes and three heat release schemes. The following key findings are derived:

(1) The integration of heat storage devices to assist with peak shaving can effectively enhance the flexibility of coal-fired power units, significantly increasing their peak shaving capacity and improving grid accommodation for renewable energy sources.

(2) Among the heat storage schemes, Scheme 1 exhibited the strongest load regulation capability, achieving a peak shaving capacity of up to 60 MW and a peak shaving depth of 9% when the heat storage power was 120 MW. Meanwhile, Scheme 3 demonstrated the highest system efficiency and economic performance. As the heat storage power increased, the unit's efficiency improved, reaching 43.3% at 120 MW, though the coal consumption rate also rose to 331 g/(kW·h).

(3) Among the heat release schemes, Scheme 1 exhibited the strongest up-peaking capability, achieving a peak shaving capacity of 15 MW and a thermoelectric conversion ratio of 30% at a heat release power of 50 MW, followed by Scheme 2, with Scheme 3 performing the worst. As the heat release power increased, the unit's thermal efficiency decreased, but its coal consumption rate also declined. Scheme 1 demonstrated the highest system efficiency and economic performance, with a thermal efficiency of 38.5% and a coal consumption per unit of electricity generation of 297 g/(kW·h) at a heat release power of 50 MW.

Acknowledgements

This study is financially supported by Inner Mongolia Autonomous Region Major Science and Technology Special Project (2021ZD0036), Inner Mongolia Autonomous Region Science and technology project (2023YFHH0070), Inner Mongolia Autonomous Region 'Open bidding for selecting the best candidates' project (2023JBGS0012), Many thanks for the help with these programs.

Reference

- [1]Zhang L., et al. Performance analysis of a compressed air energy storage system integrated into a coal-fired power plant[J]. Energy Conversion and Management, 2020, 225: 113446.
- [2]Wang J., et al. Flexibility transformation decision-making evaluation of coal-fired thermal power units deep peak shaving in China[J]. Sustainability, 2021, 13(4): 1882.
- [3]Yang K., et al. Research on capacity allocation optimization of coupling of multiple heating retrofits under deep peak shunted [J]. Journal of Engineering for Thermal Energy and Power,2024,39(09):123-133.
- [4]Huang C., et al. Study on gas-solid flow characteristics of a new low load burner with steady combustion [J/OL]. Clean Coal Technology,2024:1-11.
- [5]Meng X. Simulation and Optimization Analysis of Heat Transfer Characteristics of Molten Salt-Flue Gas Heat Exchangers in Thermal Power Plants [D]. Inner Mongolia: Inner Mongolia University of Technology, 2023.
- [6]Fan Z., et al. Analysis of zero output thermal performance, peak shaving performance and economic performance of low pressure cylinder of 300 MW heating unit [J]. China Measurement & Test,2024,50(04):166-172.

- [7]Zhang Z., et al. Application status and research progress of molten salt heat storage technology [J]. Integrated Intelligent Energy,2023,45(9):40-47.
- [8]LI J., et al. Flexibility transformation technology of thermal power unit based on high temperature molten salt heat storage and its application prospect analysis [J]. Southern Energy Construction,2021,8(03):63-70.
- [9]Zhou K., et al. Research progress of coal-fired power-physical thermal storage coupling technology and analysis of system peak shaving capacity [J]. Clean Coal Technology,2022,28(03):159-172.
- [10]Song X., et al. Comparison and analysis of depth peak shaving schemes for thermal power units based on high temperature molten salt heat storage system [J]. Journal of Engineering for Thermal Energy and Power,2023,38(11):63-74+83.
- [11]Kosman W, et al. Application of an energy storage system with molten salt to a steam turbine cycle to decrease the minimal acceptable load[J]. Energy, 2023, 266: 126480.
- [12]Liu J., et al. Design and performance comparison of peak shaving system for coal-fired unit assisted by molten salt heat storage[J]. Thermal Power Generation,2023,52(02):111-118.
- [13]Jia Z., et al. Study on peak shaving performance and thermal economy of thermal power unit coupled with molten salt heat storage system[J]. Thermal Power Generation,2024,53(10):72-80.
- [14]Holy F., et al. Gas turbine cogeneration concepts for the pressureless discharge of high temperature thermal energy storage units[J]. Journal of Energy Storage, 2021, 44: 103283.
- [15]Chen C., et al. Study of combined heat and power plant integration with thermal energy storage for operational flexibility[J]. Applied Thermal Engineering, 2023, 219: 119537.
- [16]Wei H., et al. Research on deep peak shaving and large-scale renewable energy consumption of coal-fired units based on heat storage [J]. Thermal Power Generation,2023,52(02):79-89.
- [17]Wei Q, Zheng P, Zou S, et al. Research on the combined low pressure steam bypass and heat storage peak shaving for industrial extraction steam heating units[J]. Energy Reports, 2022, 8: 179-187
- [18]Abdur Rehman O., et al. Enabling technologies for sector coupling: A review on the role of heat pumps and thermal energy storage[J]. Energies, 2021, 14(24): 8195.
- [19]Beiron J., et al. Flexible operation of a combined cycle cogeneration plant–A techno-economic assessment[J]. Applied Energy, 2020, 278: 115630.
- [20]Trojan M., et al. The use of pressure hot water storage tanks to improve the energy flexibility of the steam power unit[J]. Energy, 2019, 173: 926-936

- Paper submitted: 25 November 2024
- Paper revised: 7 March 2025
- Paper accepted: 7 March 2025